Homepage :
https://journal.ubaya.ac.id/index.php/MPI/index
DOI 10.24123/mpi.v7i2.7601

Research Article
p-ISSN 2527-6298 | e-ISSN 2527-9017

Design of Casocidin-II Mutation Variants as Antibacterial Candidates against *Helicobacter pylori* using Bioinformatic Approaches

Yulianto Ade Prasetya[1], and Tjie Kok[1,2]

[1] Faculty of Biotechnology, University of Surabaya, Surabaya, 60293, Indonesia
[2] Center of Excellence for Food Products and Health Supplements for Degenerative Conditions, University of Surabaya, Surabaya, 60293, Indonesia

Correspondence: Tjie Kok
Email: tjie_kok@staff.ubaya.ac.id

Submitted: 09-04-2025, *Revised:* 04-12-2025, *Accepted:* 04-12-2025, *Published regularly: December 2025*

ABSTRACT: *Helicobacter pylori infects about 50% of the global population, with high prevalence in Indonesia, particularly in East Nusa Tenggara (51.4%) and Papua (30.7%). If untreated, this infection can cause gastritis, ulcers, and even gastric cancer. Due to rising antibiotic resistance to this bacterium, alternative treatments are needed. Casocidin-II, an antimicrobial peptide from cows milk (Bos taurus), has antibacterial potential but it is unstable in acidic environments, making it ineffective against H. pylori, which colonizes in the stomach. This research aims to design and analyze Casocidin-II mutations using bioinformatic approaches to improve stability without reducing antibacterial activity. Mutations were conducted using I-Mutant 2.0, and structural modeling was done with PEP-FOLD4. Physicochemical properties were analyzed with ExPASy, and the binding affinity to H. pylori BabA receptor was evaluated using HADDOCK. Molecular interactions were visualized with ChimeraX. Eight stable Casocidin-II mutants (CAS1–CAS8) were identified, with CAS3 and CAS5 showing the best stability, hydrophilicity, and aliphatic index. Docking results showed CAS3 and CAS7 had the highest binding affinities, -121.70 kcal/mol and -123.24 kcal/mol, respectively. CAS3, with the sequence KTKLTVEEKNRLNFLKKISQRYQKFALPQYLKTVYQHQK, was the most effective in inhibiting H. pylori growth and is a strong candidate for further laboratory testing. Besides its high affinity and activity, CAS3's amino acid profile enhaces target binding and membrane penetration. This research demonstrates that bioinformatics can be used in designing mutation varians to enhance peptide stability and antibacterial properties. CAS3 is a promising alternative to conventional antibiotics for H. pylori treatment, pending further experimental validation.*

Keywords: *antimicrobial; Casocidin-II; Helicobacter pylori; molecular docking; mutation; peptide*

1. Introduction

Helicobacter pylori is a Gram-negative, opportunistic commensal bacterium that colonizes in the gastric mucosa of humans and is responsible for various gastrointestinal disorders, including gastritis, peptic ulcers, and gastric cancer [1]. It is estimated that approximately 50% of the global population is infected with *H. pylori*, making it a significant public health concern worldwide [2]. The prevalence of *H. pylori* infection is reported to be around 43.1%, with the highest infection rates observed among young individuals and in developing countries [3]. In Indonesia, the prevalence varies across regions, with rates of 51.4% in East Nusa Tenggara, 30.7% in Papua, 24.4% in Sumatra, 18% in Bali, 8.9% in Kalimantan, 7.4% in Java, and 4.5% in Maluku [4]. Standard treatment for *H. pylori* infection involves a combination of one or two antibiotics with proton pump inhibitors (PPIs) [5]. However, if left untreated, *H. pylori* infection can lead to chronic gastritis, peptic ulcers, duodenal ulcers, and gastric cancer [6]. Additionally, the growing resistance of *H. pylori* to antibiotics has become a major challenge, reducing the effectiveness of combination therapies [7]. Consequently, the development of new, more effective alternatives of antibacterial agents are crucial. Among these potential alternatives, antimicrobial peptides (AMPs) have emerged as promising candidates.

Antimicrobial peptides are bioactive molecules with significant potential for therapeutic applications, including their role as novel antibacterial agents [8]. These peptides exhibit broad-spectrum antibacterial activity with a lower likelihood of resistance development compared to conventional antibiotics [9]. One such peptide with substantial antibacterial potential is Casocidin-II, which is derived from the αS2-casein fragment found in bovine milk. This peptide is generated through protein hydrolysis by trypsin and is structurally identical to Casocidin-I, except for an additional amino acid at the N-terminus and seven additional amino acids at the C-terminus, spanning residues 166-196 of the protein sequence [10]. Casocidin-II demonstrates broad-spectrum antimicrobial activity against both Gram-positive and Gram-negative bacteria. Its mechanism of action involves disrupting microbial cell membranes, leading to leakage of intracellular components and ultimately resulting in pathogen cell death. Studies have shown its efficacy in inhibiting pathogenic microorganisms, including *Escherichia coli*, *Staphylococcus aureus*, and *Candida albicans* [11]. Further research has reported that Casocidin-II exhibits dose-dependent antibacterial activity, with a minimum inhibitory concentration (MIC) of 16.2 μM against *Bacillus subtilis* ATCC6051, *E. coli* ATCC25922, and *E. coli* NEB5α [10]. However, its effectiveness against *H. pylori* has not been previously explored, which is the primary focus of this study using bioinformatic approaches.

Blood Group Antigen Binding Adhesin (BabA) is a crucial outer membrane protein in *H. pylori* that plays a significant role in host colonization and pathogenesis. BabA is an adhesin, meaning it facilitates bacterial attachment to host cells by specifically binding to Lewis b (Leb) antigens present on gastric epithelial cells [12]. This binding is essential for *H. pylori* to establish a persistent infection in the harsh acidic environment of the stomach. BabA-mediated adhesion enhances bacterial survival, promotes gastric inflammation, and increases the risk of diseases such as gastritis, peptic ulcers, and gastric cancer [13]. Studies have shown that *H. pylori* strains expressing high levels of BabA, have stronger adhesion capabilities and are often associated with more severe clinical outcomes. Due to its critical role in bacterial attachment and infection, BabA has been targeted in therapeutic strategies aimed at blocking *H. pylori* adhesion, preventing colonization, and reducing bacterial persistence in the stomach. Research on BabA inhibitors, vaccines, and antimicrobial peptides continues to explore new ways to combat *H. pylori* infections, particularly in antibiotic-resistant strains [14].

One major reason why Casocidin-II has not been investigated for *H. pylori* treatment is its

susceptibility to degradation in acidic environments [15]. Since *H. pylori* colonizes the human stomach, in which the pH ranges from 1.5 to 3.5, any potential therapeutic peptide must exhibit acid stability. Therefore, bioinformatics-driven protein mutation design using I-Mutant 2.0 is essential to assess the pH stability of this peptide in acidic conditions. Further molecular docking, dynamic simulations, and sequence optimization can help predict the structural and functional effects of specific mutations. This approach aims to enhance Casocidin-II's binding affinity, stability, and antibacterial activity against *H. pylori* in BabA, paving the way for the development of a novel antimicrobial peptide-based therapy. This research aims to design and analyze Casocidin-II mutation variants using a bioinformatics approach as an antibacterial candidate against *H. pylori* infection.

2. Materials and methods

2.1. Protein sequence dataset

The Casocidin-II structure was downloaded in PDB format from the Protein Data Bank under the accession code 6FS5 (resolution of 2.96 Å). It was ensured that the peptide structure was complete, including all necessary residues and atomic details required for the mutation process.

2.2. Stability analysis of mutations using I-Mutant 2.0

The I-Mutant 2.0 software was used to analyze the effects of mutations on protein stability [16]. The Casocidin-II structure in PDB format was loaded, and its sequence was examined. The I-Mutant 2.0 settings were adjusted to a pH of 2 and a temperature of 37°C. Predictive simulations were performed to evaluate the stability of mutations with relevant residue variations, and changes in Gibbs free energy (ΔG) were recorded to determine whether the mutations increased or decreased stability. Single-point mutations that resulted in improved stability and a reliability index greater than 5 were selected for further analysis.

2.3. Structural modeling of mutated Casocidin-II using PEP-FOLD4

The modified Casocidin-II peptide sequences were submitted to PEP-FOLD4 for 3D structure prediction [17]. The pH was set to 2 to simulate the gastric environment. The most probable conformations of the mutated peptides were generated, and the best structural model was saved in PDB format for further analysis. The downloaded PDB files were then opened in ChimeraX, where water molecules were removed to optimize the structure for subsequent docking studies.

2.4. Physicochemical analysis using ExPASy ProtParam

The qualitative identification of Casocidin-II sequences began with preparing the protein sequence data in FASTA format. The ExPASy website (https://www.expasy.org/) was accessed to perform relevant protein sequence analyses using ProtParam [18]. The Casocidin-II sequence was either directly input into the tool or uploaded if a compatible file format was available. ProtParam was used to analyze physicochemical properties, including molecular weight, isoelectric point (pI), protein stability, and hydrophobicity index. These results provided an initial assessment of the stability and activity potential of the mutated peptides. The ProtParam analysis results were reviewed to understand the qualitative characteristics of Casocidin-II and their compatibility with the designed mutations. All data were recorded for further evaluation and to support future experimental validation of protein activity.

2.5. Molecular docking with BabA (4Z7H) using HADDOCK

The 3D structure of BabA (PDB ID: 4Z7H) was downloaded from the Protein Data Bank. Both BabA and peptide models were cleaned in ChimeraX by removing solvent molecules and correcting missing atoms. Active residues on BabA were selected based on published interaction sites related to gastric mucin adhesion, while peptide active residues were derived from structural ex-

posure analysis. Protein–peptide docking was performed using HADDOCK 2.4 with default parameters [19]. Docking scores, van der Waals energy, electrostatic energy, and buried surface area (BSA) were used for ranking.

2.6. Visualization of docking results using ChimeraX

The visualization of docking results was carried out using ChimeraX to examine residue interactions, including hydrogen bonds, electrostatic interactions, and hydrophobic contacts [20]. The most stable protein-peptide complex was selected for further analysis, and key interacting residues were marked. The effects of mutations on binding affinity were evaluated by comparing interactions with the wild-type Casocidin-II. This simulation was used to identify the most promising Casocidin-II mutant with optimal binding affinity and antibacterial potential against *H. pylori*. Final docking results were saved and visualized for documentation and advanced analysis. By applying this method, PyMOL-assisted docking simulations provided a detailed evaluation of the most potent peptide mutations, facilitating the identification of optimal antibacterial candidates against *H. pylori*.

2.7. Molecular dynamics simulation using Galaxy–RefineMD

Molecular dynamics (MD) simulations were performed to validate the structural stability of the most promising mutant, CAS3. The three-dimensional structure generated using PEP-FOLD4 was used as the initial model and submitted to the GalaxyRefineMD server (https://galaxy.seoklab.org/). The peptide structure was placed in an explicit TIP3P water environment using a cubic simulation box with a 10 Å buffer distance, and the CHARMM36 force field was applied throughout the simulation. Prior to the production run, the system underwent 5,000 steps of energy minimization followed by equilibration under NVT conditions for 100 ps and NPT conditions for 200 ps to ensure temperature and pressure stabilization at 310 K. A 10-ns production simulation was subsequently conducted to assess the dynamic behavior of CAS3 under physiologically relevant conditions. The resulting trajectories were analyzed to evaluate root-mean-square deviation (RMSD), root-mean-square fluctuation (RMSF), radius of gyration (Rg), solvent-accessible surface area (SASA), and intramolecular hydrogen bonding patterns. These parameters collectively provided insight into the conformational stability, structural compactness, and dynamic flexibility of CAS3 along the simulation timeline.

3. Results and discussion

3.1. Stability of Casocidin-II mutations

The results of Casocidin-II mutations using I-Mutant 2.0 (Table 1) against BabA identified eight mutation variants designed to optimize interactions with the target protein BabA (PDB ID: 4ZH0). Each mutation involved substituting a wild-type (WT) residue with a new residue (NEW) at a specific position, with varying relevance index (RI) values. A mutation at position 1 (K → V), the substitution of lysine with valine produced an RI value of 8, indicating enhanced interaction potential due to hydrophobic effects. At position 3 (K → P), the substitution of lysine with proline resulted in an RI value of 7, suggesting reduced flexibility due to proline's rigid structure. A mutation at position 6 (E → V) had an RI of 6, suggesting that substituting glutamic acid with valine produced a minor effect. At position 10, the substitution of asparagine with either valine (N → V) or isoleucine (N → I) yielded an RI of 9 and 8, respectively, indicated a significant role in BabA interaction.

The mutation at position 19 (S → F) gave RI of 7 showing that replacing the hydrophilic serine with hydrophobic phenylalanine had a moderate impact on interaction. At position 24, the substitution of lysine with valine (K → V), the highest RI value of 9 was observed, suggesting that this residue played a crucial role in interaction, likely due to its change from positively charged to hy-

Table 1. Casocidin-II mutation results at pH 2 and 37°C using I-Mutant 2.0

Code	Position	WT	NEW	RI	Mutated sequence
CAS1	1	K	V	8	VTKLTEEEKNRLNFLKKISQRYQKFALPQYLKTVYQHQK
CAS2	3	K	P	7	KTPLTEEKNRLNFLKKISQRYQKFALPQYLKTVYQHQK
CAS3	6	E	V	6	KTKLTVEEKNRLNFLKKISQRYQKFALPQYLKTVYQHQK
CAS4	10	N	V	9	KTKLTEEEKVRLNFLKKISQRYQKFALPQYLKTVYQHQK
CAS5	10	N	I	8	KTKLTEEEKIRLNFLKKISQRYQKFALPQYLKTVYQHQK
CAS6	19	S	F	7	KTKLTEEEKNRLNFLKKIFQRYQKFALPQYLKTVYQHQK
CAS7	24	K	V	9	KTKLTEEEKNRLNFLKKISQRYQVFALPQYLKTVYQHQK
CAS8	30	Y	F	6	KTKLTEEEKNRLNFLKKISQRYQKFALPQYLKTVFQHQK

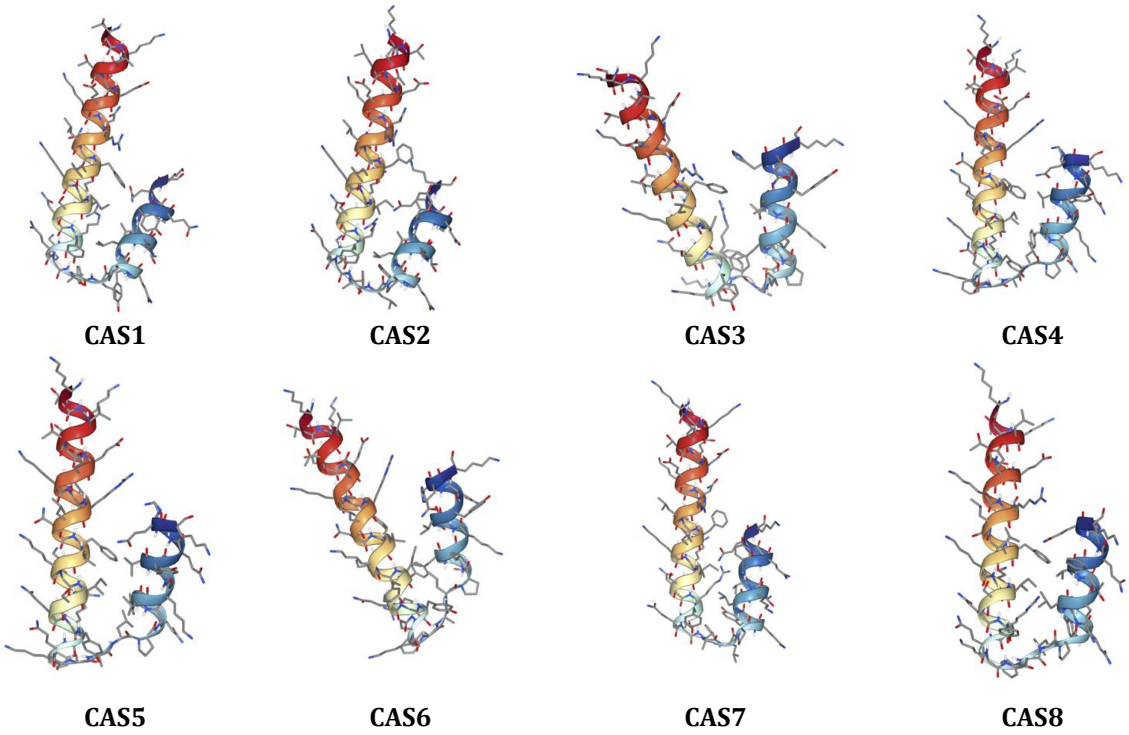

Figure 1. The three-dimensional (3D) structural prediction of the mutant Casocidin-II peptides (CAS1-CAS8) generated using PEP-FOLD4

drophobic. Finally, the mutation at position 30 resulted in RI of 6, suggesting that substituting tyrosine with phenylalanine (Y → F) had a relatively minor effect.

Overall, mutations at positions 10 and 24 with the highest RI values presented the greatest potential for enhancing Casocidin-II interactions with BabA. The change in RI values also indicated that converting hydrophilic or charged residues into hydrophobic ones could strengthen interactions. These findings provide a foundation for further docking simulations and future experimental validation, focusing on mutations with the highest antibacterial potential against *H. pylori*.

3.2. Structural modeling of Casocidin-II mutations

The three-dimensional (3D) structure predictions of the Casocidin-II mutants (CAS1 to CAS8) using PEP-FOLD4 (Figure 1) revealed conformational variations depending on specific residue substitutions. These structures were represented as ribbon models, with gradient coloring indicating secondary structure elements such as stable α-helices (red/orange) and flexible loops (blue).

CAS1, the wild-type (WT) Casocidin-II, exhibited a dominant α-helix structure, with flexible loops at the N-terminal and C-terminal ends, serving as a reference for comparison with the mutated variants. CAS2 and CAS3 mutations maintained α-helix stability, indicating that these mutations did not significantly impact structural integrity. However, CAS4 and CAS5 exhibited minor disruptions in the central α-helix, while CAS6, CAS7 and CAS8 displayed greater conformational variations with increased loop flexibility, potentially influencing interactions with the target protein. Red and orange regions in the structure indicated highly stable α-helices, essential for protein-peptide interactions, while blue regions denoted high flexibility, commonly found in loops or terminal ends, allowing adaptability to binding targets. CAS2 and CAS3, which retained an intact α-helix structure, showed high potential for optimal interaction with BabA, whereas the higher flexibility in CAS6 to CAS8 might provide advantages in binding adaptation but reduce overall stability.

The conformational prediction for the eight mutant variants of Casocidin-II (CAS1 to CAS8) generated using PEP-FOLD4 was represented by the heatmap (Figure 2). The colors on the heatmap indicate the probability of residue-residue interactions within the peptide structure. Green regions (high probability, 0.8–1.0) indicate strong residue interactions, typically associated with structurally stable α-helices**.** Blue regions (moderate probability, 0.4–0.8) represent moderate interactions, often related to residue flexibility**.** Red regions (low probability, 0.0–0.4) indicate areas with high flexibility or weak interactions, which are usually found at the N-terminal or C-terminal ends and flexible loops.

CAS1 (wild type) predominantly exhibits green regions in the central part, indicating high stability in the main α-helix structure, while the N-terminal and C-terminal ends appear red, showing high flexibility, which is typical for terminal residues. CAS2 and CAS3, which underwent mutations, maintain an interaction pattern like CAS1, suggesting that these mutations did not significantly alter the stability of the primary structure. In CAS4 and CAS5**,** a slight reduction in green areas in the central region indicates that mutations moderately affected α-helix stability. CAS6 to CAS8 show an increase in red areas, especially at the terminal and loop regions, suggesting that these mutations introduced higher flexibility, which could influence the peptides interaction potential with the target protein.

3.3. Qualitative sequence analysis of Casocidin-II mutants

The physicochemical properties of Casocidin-II mutants (CAS1–CAS8) were analyzed, including molecular weight, theoretical isoelectric point (pI), instability index, aliphatic index, and grand average of hydropathicity (GRAVY) (Table 2). The molecular weight of the mutants ranged from 4709.52 to 4929.79 Da, reflecting slight mass variations due to residue substitutions. CAS6 had the highest molecular weight (4929.79 Da), likely due to larger side-chain residues. The isoelectric point (pI) ranged between 10.00 and 10.24, indicating that all variants were basic peptides, with positively charged residues facilitating interactions in acidic gastric environments (pH ~2). CAS3 (pI = 10.24) and CAS8 (pI = 10.17) exhibited slightly higher values, contributing to enhanced stability in acidic conditions.

The instability index, predicting protein stability in solution, showed that CAS3 was the most stable with an instability index of 14.56, while CAS8 had the highest instability index of 29.79 but remained within the stable range. The aliphatic index, reflecting thermal stability, was highest in CAS5 (80.00), suggesting better stability at varying temperatures. CAS6 and CAS8 had the lowest values (70.00), indicating potentially lower thermal stability. The GRAVY score, indicating hydrophilicity, was negative for all variants (-1.118 to -1.233), confirming that all peptides were hydrophilic. CAS6 had the lowest GRAVY score of -1.233, meaning it was the most hydrophilic, enhancing solubility in aqueous environments, crucial for interaction with BabA in

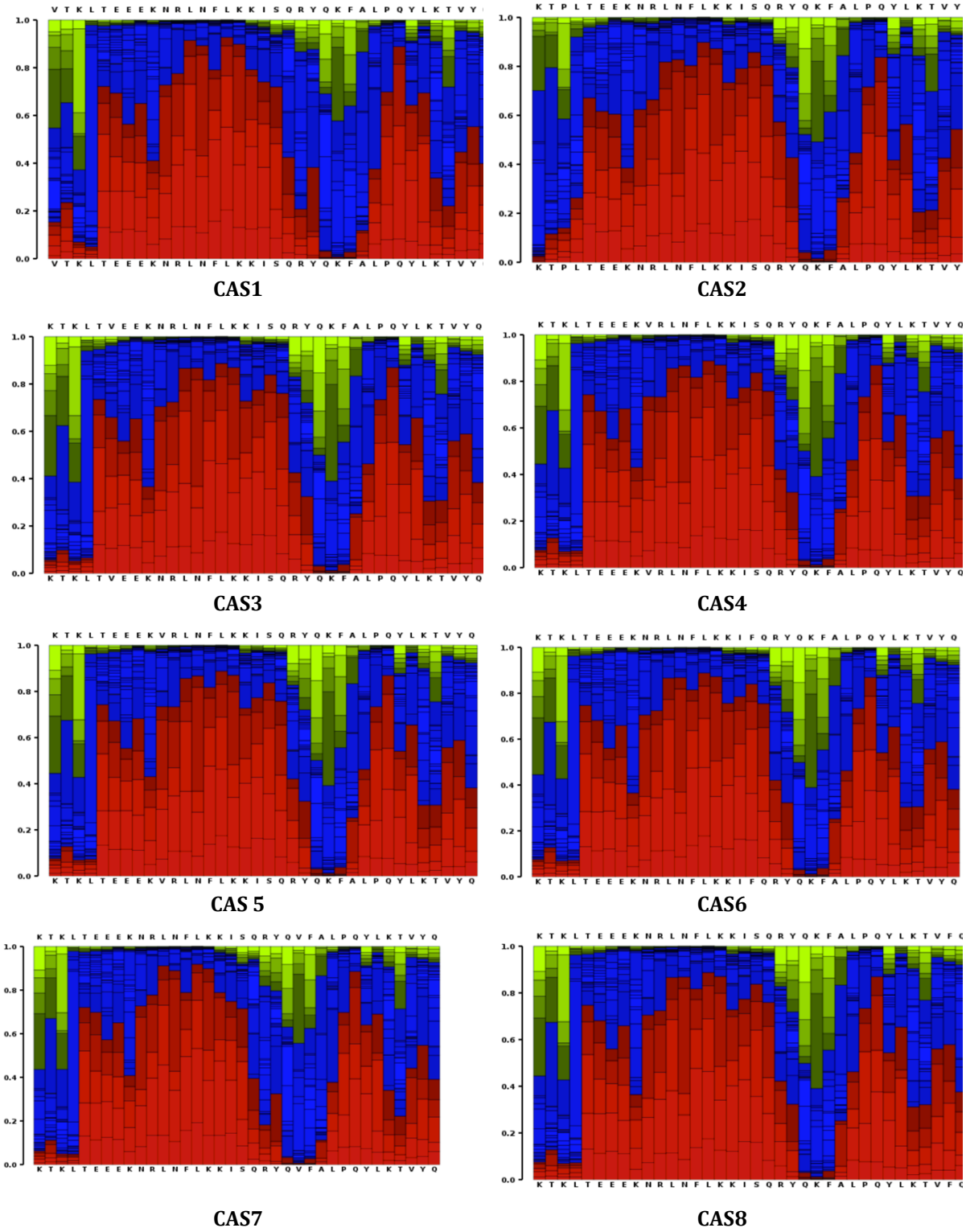

Figure 2. Heatmap of the conformational predictions for the eight mutant variants of Casocidin-II (CAS1–CAS8) generated using PEP-FOLD4

the stomach. Overall, CAS3 and CAS5 exhibited the most optimal physicochemical properties, including high stability, high aliphatic index, and strong hydrophilicity, making them strong candidates for antibacterial testing against *H. pylori*.

3.4. Identification of Casocidin-II mutant interactions with BabA

The docking analysis of Casocidin-II mutations (CAS1–CAS8) revealed differences in key parameters, including RMSD, van der Waals energy,

Table 2. Physicochemical properties of Casocidin-II mutants (CAS1–CAS8) using ProtParam

Code	Molecular weight (Da)	Theoretical pI	Instability index	Aliphatic index	GRAVY
CAS1	4840.65	10.00	25.68	77.44	-1.118
CAS2	4709.52	10.17	21.98	71.84	-1.208
CAS3	4839.71	10.24	14.56	77.44	-1.128
CAS4	4854.72	10.08	25.68	77.44	-1.128
CAS5	4868.75	10.08	25.68	80.00	-1.121
CAS6	4929.79	10.08	22.92	70.00	-1.233
CAS7	4840.65	10.00	25.92	77.44	-1.118
CAS8	4853.69	10.17	29.79	70.00	-1.221

Table 3. Docking results between the mutant Casocidin-II peptide and *H. pylori* BabA

Characteristics	Mutant code							
	CAS1	CAS 2	CAS 3	CAS 4	CAS 5	CAS 6	CAS 7	CAS 8
RMSD from the overall lowest-energy structure (Å)	0.3 ± 0.2	0.4 ± 0.3	0.6 ± 0.4	8.9 ± 0.2	8.7 ± 0.1	1.4 ± 0.8	2.4 ± 0.1	9.0 ± 0.1
Van der Walls energy (kcal/mol)	-61.5 ± 2.7	-67.5 ± 11.7	-70.3 ± 6.0	-65.6 ± 5.0	-66.9 ± 3.6	-60.7 ± 10.0	-67.5 ± 4.2	-67.1 ± 4.2
Burried surface area (BSA) (Å^2)	1912.7	1797.1	1920.7	1851.7	1853.0 ± 80.1	1877.8	1849.5	1869.4
Z-score	-1.9	-2.3	-2.3	-2.4	-1.7	-2.1	-1.9	-2.7

buried surface area, and Z-score (Table 3). CAS1 had an RMSD of 0.3 ± 0.2 Å, indicating minimal structural deviation and high structural stability. Its van der Waals energy was -61.5 ± 2.7 kcal/mol, suggesting moderate interaction with BabA, while the buried surface area (BSA) of 1912.7 ± 132.1 Å^2 reflected extensive ligand-protein contact. Its Z-score of -1.9 indicated good overall stability of the complex.

CAS2 had an RMSD of 0.4 ± 0.3 Å, slightly higher than CAS1 but still within a stable structural range. Its van der Waals energy of -67.5 ± 11.7 kcal/mol was lower than CAS1, indicating stronger interaction. However, its BSA of 1797.1 ± 103.2 Å^2 was slightly lower than CAS1, and the Z-score of -2.3 suggested moderate stability. CAS3 emerged as the best candidate with an RMSD of 0.6 ± 0.4 Å, which, while higher than CAS1 and CAS2, remained within acceptable stability limits. Its van der Waals energy of -70.3 ± 6.1 kcal/mol was the lowest (most negative), indicating the strongest van der Waals interactions among all mutations. Additionally, its BSA of 1920.7 ± 106.9 Å^2 was the largest, confirming optimal ligand-protein contact, while its Z-score of -2.3 reinforced the overall stability. Conversely, CAS4 exhibited a very high RMSD of 8.9 ± 0.2 Å, suggesting structural instability. Its van der Waals energy of -65.6 ± 5.0 kcal/mol was decent but not as optimal as CAS3, while its BSA of 1851.7 ± 117.9 Å^2 was at a moderate level. The Z-score of -2.4 indicated low stability.

Similarly, CAS5 had a high RMSD of 8.7 ± 0.1 Å, indicating significant structural instability. Its van der Waals energy of -66.9 ± 3.6 kcal/mol reflected moderate interaction strength, while its BSA of 1853.0 ± 80.1 Å^2 was in the mid-range. The Z-score of -1.7 was the highest among all mutations, but it did not indicate optimal interaction stability. CAS6 displayed an RMSD of 1.4 ± 0.8 Å, signifying better stability than CAS4 and CAS5. However, its van der Waals energy of -60.7

± 10.0 kcal/mol was the weakest, making it the least favorable interaction among the mutations. The BSA of 1877.8 ± 98.5 Å^2 was moderate, while the Z-score of -2.1 reflected fair overall stabi–lity. CAS7 had an RMSD of 2.4 ± 0.1 Å, which was higher than CAS1–CAS3 but remained within an accep–table stability range. Its van der Waals energy of -67.5 ± 4.2 kcal/mol indicated strong interactions, while its BSA of 1849.5 ± 78.3 Å^2 was mode–rate. The Z-score of -1.9 suggested good overall stability. CAS8 exhibited the highest RMSD of 9.0 ± 0.1 Å, indicating significant struc-tural instabi–lity. Its van der Waals energy of -67.1 ± 4.2 kcal/mol was strong but not optimal, while its BSA of 1869.4 ± 120.2 Å^2 was mode–rate. The Z-score of -2.7 was the lowest, indicating poor overall stability.

Based on this analysis, CAS3 emerged as the best mutation due to its lowest van der Waals energy of -70.3 ± 6.1 kcal/mol, largest buried surface area of 1920.7 ± 106.9 Å^2, and a stable Z-score of -2.3. The strong van der Waals inter-actions and extensive ligand-protein contact sug-gest that CAS3 has the highest affinity and most stable interaction with BabA, making it the most promising candidate for further validation and antibacterial testing against *H. pylori* [15].

3.5. Visualization of Casocidin-II mutant docking (CAS1–CAS8) with H. pylori BabA

The docking visualization of Casocidin-II mu-tants (CAS1–CAS8) with BabA protein revealed differences in ligand positioning and molecular interactions at the binding site (Figure 3). CAS1 and CAS8 exhibited the strongest interactions, forming a significant number of hydrogen bonds, indicating high stability within the binding pocket. CAS1 demonstrated a stable ligand position with strong hydrogen bonding at key residues, while CAS8 formed the highest number of hydrogen bonds, making it a strong potential candidate for BabA interaction. CAS3 and CAS7 showed opti-mal aromatic ring orientation for hydrophobic interactions, though they formed fewer hydrogen bonds, which could impact long-term interaction stability. CAS5 displayed high ligand flexibility but weaker interactions compared to the other muta-tions. Based on this analysis, CAS1 and CAS8 were identified as the best candidates for further in-vestigation due to their strong hydrogen bonding interactions and stable ligand orientation, alig–ning with high-affinity criteria for ligand binding in protein-peptide docking studies.The docking results for Casocidin-II mutations (CAS1–CAS8) with BabA protein demonstrated variations in binding affinity scores, solvation energy, and inte–racting residues (Table 4). CAS1 had a binding af-finity score of -107.07 kcal/mol and a solvation energy of -6.229 kcal/mol, with interactions at L-15 (Leucine), a hydrophobic residue contribu–ting to interaction stability. CAS2 showed a bin–ding affinity of -107.65 kcal/mol and a solvation energy of -6.222 kcal/mol, interacting with S-53 (Serine) and K-51 (Lysine), which are polar and positively charged residues, providing mode–rate stability. CAS3 exhibited a binding affinity of -121.70 kcal/mol, one of the strongest interac-tions, with N-369 (Asparagine), a polar residue, although its solvation energy of -6.155 kcal/mol was slightly higher than other mutations. CAS4 had the lowest binding affinity of -102.15 kcal/mol and a solvation energy of -5.856 kcal/mol, interacting with N-509 (Asparagine), suggesting weak interaction stability.

CAS5 recorded a binding affinity of -109.34 kcal/mol and the best solvation energy of -6.461 kcal/mol among all mutations, interacting with E-469 (Glutamate), a negatively charged resi-due, indicating high stability in hydrated envi-ronments. CAS6 had a binding affinity of -105.00 kcal/mol and a solvation energy of -6.274 kcal/mol, interacting with I-50 (Isoleucine), a hydro-phobic residue, although its interaction strength was lower than CAS3 and CAS7. CAS7 emerged as the best mutation, with the most negative binding affinity of -123.24 kcal/mol and a solvation ener–gy of -6.166 kcal/mol, interacting with Q-451 (Glutamine), a polar residue. This indicates that CAS7 exhibits the strongest and most stable in-teraction within the BabA active site.

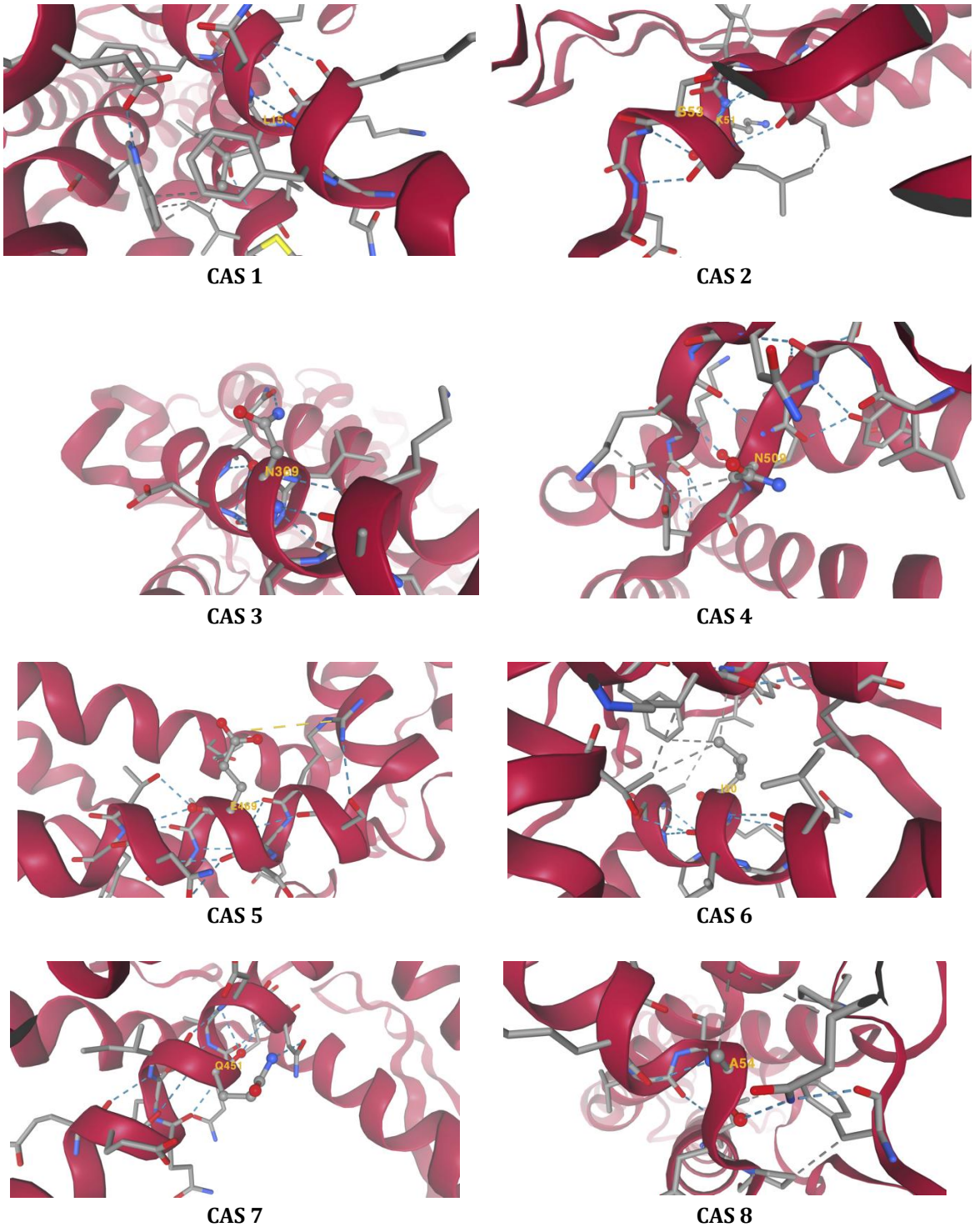

Figure 3. Visualization results of CAS1–CAS8 mutant docking with BabA

Table 4. Docking analysis results of CAS1-CAS8 mutant with BabA

Characteristics	Mutant code							
	CAS1	CAS2	CAS3	CAS4	CAS5	CAS6	CAS7	CAS8
Binding affinity (kcal/mol)	-107.07	-107.65	-121.70	-102.15	-109.34	-105.00	-123.24	-119.20
Solvation energy (kcal/mol)	-6.229	-6.222	-6.155	-5.856	-6.461	-6.274	-6.166	-5.831
Ligan-receptor interaction residues	L-15	S53 and K51	N-369	N-509	E-469	I-50	Q-451	A-54

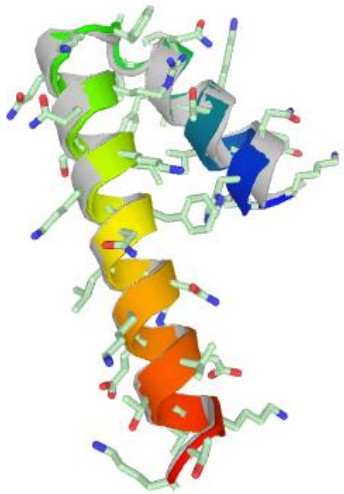

Figure 4. Final MD-equilibrated conformation of the Casocidin-II mutant, showing a stable α-helical structure

Table 5. Structural validation molecular dynamics of CAS-3 by GalaxyRefine

Parameter	Refined structure
RMSD (Å)	0.644
MolProbity	0.633
Clash score (per 100 atoms)	0.0
Poor rotamers (%)	0.0
Rama favored (%)	100.0
Galaxy energy (arbitrary units)	-1068.53

Although CAS8 had the second-best binding affinity of -119.20 kcal/mol, its solvation energy (-5.831 kcal/mol) was higher and it interacted with A-54 (Alanine), a nonpolar residue. Based on this analysis, CAS7 was identified as the most promising candidate, as it exhibited the lowest (most negative) binding affinity of -123.24 kcal/mol, strong interaction with the key polar residue Q-451, and solvation energy that supports stability in biological environments [15].

Hydrogen bond interaction were also confirmed at the residual level. CAS1 formed hydrogen bonds with residues L15 and nearby polar residues, while CAS8 demonstrated multiple hydrogen bonds involving backbone interactions within the BabA binding pocket. In CAS3, hydrogen bonding with N369 contributed to its high binding affinity. These residue-level interaction clarify the molecular basis of mutant peptide stability within the active site.

3.6. Molecular dynamics simulation

The structural refinement analysis produced by GalaxyRefine (Figure 4) demonstrated substantial improvements in stereochemical quality and stability across the predicted peptide models. Compared with the initial structure—which exhibited a high MolProbity score, severe steric clashes, and extremely unfavorable energy—the refined models showed markedly enhanced backbone geometry, zero rotamer outliers, and near-complete Ramachandran favored distributions, consistent with high-quality peptide conformations as recommended in modern structural validation standards (Table 5). The structure was characterized by a low RMSD (0.644 Å), optimal MolProbity score (0.500), absence of ste-

ric clashes, 100% Rama–chandran favored residues, and a substantially improved energy state, making it the most reliable structure for downstream computational analyses. These findings align with recent studies demonstrating that refinement-driven side-chain repacking and local relaxation—such as those implemented in GalaxyRefine—significantly enhance peptide model accuracy and reduce structural artifacts [21,22]. Despite the comprehensive *in silico* studies, further *in vitro* and *in vivo* validation is needed to confirm the biological activity, stability, and anti *H. pylori* potential of CAS3.

4. Conclusions

Based on the results, eight optimal mutant variants (CAS1–CAS8) were identified, exhibiting enhanced stability with reliability indices ranging from 6 to 9. CAS3 and CAS5 demonstrated the most optimal physicochemical properties, including high stability (low instability index), a high aliphatic index, and strong hydrophilicity, as determined through ExPASy analysis. Docking results using HADDOCK showed that CAS3 and CAS7 had the highest binding affinity of -121.70 kcal/mol and -123.24 kcal/mol, respectively. Altogether, CAS3 emerged as the most effective mutant in inhibiting the growth of *H. pylori*. Experimental assays including minimum inhibitory concentration (MIC) testing, adhesion inhibition, and animal model studies are essential to support its translational feasibility.

References

1. Crowe SE. *Helicobacter pylori* infection. Solomon CG, editor. *N Engl J Med*. 2019;380(12):1158–65.
2. O'Connor A, O'Morain CA, Ford AC. Population screening and treatment of *Helicobacter pylori* infection. *Nat Rev Gastroenterol Hepatol*. 2017;14(4):230–40.
3. Shakir SM, Shakir FA, Couturier MR. Updates to the Diagnosis and Clinical Management of *Helicobacter pylori* Infections. *Clin Chem.* 2023;69(8):869–80.
4. Maulahela H, Doohan D, Rezkhita YAA, Syam AF, Waskito LA, Savitri CMA, et al. Infection risk in Eastern region population. 2024.
5. Ierardi E, Losurdo G, Fortezza RFL, Principi M, Barone M, Leo AD. Optimizing proton pump inhibitors in *Helicobacter pylori* treatment: Old and new tricks to improve effectiveness. *World J Gastroenterol*. 2019;25(34):5097–104.
6. Ruiz-Narváez CE, Martínez-Rodríguez JE, Cedeño-Burbano AA, Erazo-Tapia JM, Pabón-Fernández CD, Unigarro-Benavides LV, et al. *Helicobacter pylori*, úlcera péptica y cáncer gástrico. *Rev Fac Med*. 2018;66(1):103–6.
7. Tshibangu-Kabamba E, Yamaoka Y. *Helicobacter pylori* infection and antibiotic resistance — from biology to clinical implications. *Nat Rev Gastroenterol Hepatol*. 2021;18(9):613–29.
8. Luo Y, Song Y. Mechanism of Antimicrobial peptides: Antimicrobial, anti-inflammatory and anti–biofilm activities. *Int J Mol Sci*. 2021;22(21):11401.
9. Fry DE. Antimicrobial peptides. *Surg Infect*. 2018;19(8):804–11.
10. Mercurio FA, Scaloni A, Caira S, Leone M. The antimicrobial peptides casocidins I and II: Solution structural studies in water and different membrane-mimetic environments. *Peptides*. 2019;114: 50–8.
11. Benkerroum N. Antimicrobial peptides generated from milk proteins: a survey and prospects for application in the food industry. A review. *Int J Dairy Technol*. 2010;63(3):320–38.
12. Ansari S, Yamaoka Y. *Helicobacter pylori* BabA in adaptation for gastric colonization. *World J Gastroenterol*. 2017;23(23):4158.
13. Su YL, Huang HL, Huang BS, Chen PC, Chen CS, Wang HL, et al. Combination of OipA, BabA, and SabA as candidate biomarkers for predicting *Helicobacter pylori*-related gastric cancer. *Sci Rep*. 2016;6(1):36442.
14. Doohan D, Rezkitha YAA, Waskito LA, Yamaoka Y, Miftahussurur M. *Helicobacter pylori* BabA–SabA key roles in the adherence phase: The synergic mechanism for successful colonization and di–

sease development. *Toxins*. 2021;13(7):485.

15. Xiang JH, Zeng FG, Liang HZ, Sun BL, Zhang L, Li MF, et al. Model construction of the macromolecular structure of Yanzhou Coal and its molecular simulation. *J Fuel Chem Technol*. 2011;39(7):481–8.
16. Capriotti E, Fariselli P, Casadio R. I-Mutant2.0: Predicting stability changes upon mutation from the protein sequence or structure. *Nucleic Acids Research*. 2005;33.
17. Rey J, Murail S, de Vries S, Derreumaux P, Tuffery P. PEP-Fold4: A pH-dependent force field for peptide structure predicition in aqueous solution. *Nucleic Acid Res*. 2023.
18. Gasteiger E, Hoogland C, Gattiker A, Duvaud SE, Wilkins MR, Appel RD, Bairoch A. Protein identification and analysis tools on the ExPASy server. *The proteomics protocols handbook*. 2005;571-607.
19. Van Zundert GCP, Rodrigues JPGLM, Trellet M, Schmitz C, Kastritis PL, Karaca E, Melquiond ASJ, van Dijk M, de Vries SJ, Bonvin AMJJ. The HADDOCK2. 2 web server: User-friendly integrative modeling of biomolecular complexes. *Journal of molecular biology*. 2016;428(4):720-5.
20. Pettersen EF, Goddard TD, Huang CC, Meng EC, Couch GS, Croll TI, et al. UCSF ChimeraX: Structure visualization for researchers, educators, and developers. *Protein science*. 2021;30(1):70-82.
21. Heo L, Seok C. GalaxyRefine: protein structure refinement driven by side-chain repacking and molecular dynamics. *Nucleic Acids Research*. 2015;43(W1):W113–W117.
22. Williams CJ, Headd JJ, Moriarty NW, Prisant MG, Videau LL, Deis LN, et al. MolProbity: More and better reference data for improved all-atom structure validation. *Protein Science*. 2018;*27*(1):293-315.